NJC

Accepted Manuscript

This article can be cited before page numbers have been issued, to do this please use: N. Ditaranto, I. D. van der Werf, R. A. Picca, M. C. Sportelli, L. C. Giannossa, E. Bonerba, G. Tantillo and L. Sabbatini, *New J. Chem.*, 2015, DOI: 10.1039/C5NJ00527B.

ROYAL SOCIETY OF CHEMISTRY

www.rsc.org/njc

View Article Online
DOI: 10.1039/C5NJ00527B

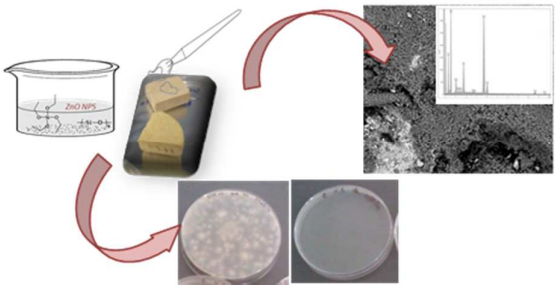

Bioactive ZnO nanoparticles embedded in polymer matrices are capable to exert a marked biological activity without changing their consolidant/water repellent properties.

View Article Online
DOI: 10.1039/C5NJ00527B

Journal Name RSCPublishing

ARTICLE

Cite this: DOI: 10.1039/x0xx00000x

Received 00th January 2012,
Accepted 00th January 2012

DOI: 10.1039/x0xx00000x

www.rsc.org/

Characterization and behaviour of ZnO-based nanocomposites designed for the control of biodeterioration of patrimonial stoneworks

Nicoletta Ditaranto[1,2*], Inez Dorothé van der Werf[1*], Rosaria Anna Picca[1], Maria Chiara Sportelli[1], Lorena Carla Giannossa[1], Elisabetta Bonerba[3], Giuseppina Tantillo[3], Luigia Sabbatini[1,2]

In this study a preventive method to fight bio-deterioration of stone substrates is proposed. It is based on the use of bioactive zinc oxide nanoparticles (ZnO-NPs) capable to exert a marked biological activity over a long period of time thanks to their peculiar structure. ZnO-NPs are synthesised by means of a simple and reproducible electrochemical procedure. The nanomaterials are embedded in consolidant/water repellent matrices to obtain nanostructured coatings. Commonly used products based on tetraethoxysilane and/or polysiloxanes were tested. The resulting nanomaterials were fully characterised with X-ray Photoelectron Spectroscopy (XPS) to investigate the amount and speciation of the NPs and the behaviour of the nanocomposites. Inductively Coupled Plasma Mass Spectrometry (ICP-MS) was used for the study of the metal release from the composites when put in contact with artificial rain water. The nanocomposites were applied on specimens composed of three different types of stone, and chromatic changes upon curing were measured with spectrophotocolorimetry. Finally, a morphological characterization by means of Scanning Electron Microscopy (SEM) was performed. ZnO-NPs nanocomposites bioactivity was also assessed in preliminary tests against *Aspergillus niger* fungus.

Introduction

Bio-deterioration of stone substrates is of great concern due to chemical-physical and aesthetic damages. The prevalently outdoor location of the majority of this type of artefacts requires a continuous maintenance, mainly consisting of periodical cleaning treatments. This implicates high costs and stress for the constitutive materials. So far, conservation strategies usually rely on the use of water repellents to reduce bioreceptivity and on the application of biocidal products to remove the biofilm and to inhibit biological activity for some time. Recently, metal oxide nanoparticles are receiving increased attention as antimicrobial agents [1-5]. These materials have longer life times as compared to organic antimicrobial agents and are chemically stable in extreme conditions. Moreover, these nanomaterials attack a broad range of targets in microorganisms, thus avoiding the development of resistance [6]. Among these, zinc oxide nanoparticles (ZnO-NPs) have attracted the interest of the scientific community for their multi-functional properties: biocompatibility, bioactivity, chemical stability. With regard to the bioactivity, ZnO-NPs have been demonstrated to be effective in killing both Gram positive and Gram negative bacteria and also in inhibiting the growth of fungi [7, 8]. Although there are many studies on the antibacterial properties of zinc nanoparticles, the mechanism of their antibacterial action is still not completely understood. In some papers it has been ascribed to the action of reactive oxygen species that are formed on the ZnO–NPs surface by a photocatalytic process [9, 10], other authors report that the antibacterial effect is related to the abrasiveness of the ZnO–NPs due to surface defects [11] or that the ZnO toxicity should be attributed to Zn^{2+} release from the nanoparticles [12, 13]. A very recent study demonstrated the combined effect of the oxidative stress caused by both ZnO-NPs and the Zn^{2+} concentration accumulated in the cell wall [14]. Even though the mechanism of action needs to be deeply investigated, ZnO-NPs have found application as antimicrobial agent in many fields. To the best of our knowledge, only one recent paper reports their use in cultural heritage preservation; specifically, ZnO-NPs are employed in the surface treatment of oil paintings to fight fungi proliferation [15]. The aim of this study is to investigate the use of ZnO-NPs mixed to state-of-the-art consolidant/water repellent materials. The idea is to exploit the

ARTICLE
View Article Online
DOI: 10.1039/C5NJ00527B
Journal Name

combined action of zinc oxide nanoparticles bioactivity and the conservation properties of the matrices, without affecting the aesthetics or being harmful to the stone substrates.

Concerning the consolidant/water repellents that were employed in this study, we have chosen commercial silicon-based products that have been widely used for about thirty years as protective and consolidating agents to preserve stone materials from decay. The advantages of this type of materials are related to good chemical stability, low surface tension, good elasticity, and resistance to thermal stress [16]. As to the influence of these materials, in particular of tetraethoxysilanes, on the porosity of treated stones, several studies are dedicated to this problem [17-19]. Indeed, restorers should be well aware of all possible advantages and drawbacks related to the use of these materials in conservation treatments, taking into account the specific properties and characteristics (composition, type of porosity, degree and type of decay, etc) of the stone substrate to be treated. In particular, the pore structure may strongly influence the water movement and thus decay phenomena such as salt crystallization, biodeterioration, freeze-thaw processes etc. [20].

In this study three commercially available consolidants/water repellents were selected (Estel1000, Silo111, and Estel1100) for the development of a bioactive nanocomposite system capable of preventing biological decay. The innovative composite materials are designed to exhibit a controlled release of the active component in order to assure a long lasting efficacy against re-colonization of stone substrates. Previously, the Authors reported on the development of nanocomposites obtained by embedding copper nanoparticles (Cu-NPs) in commercially available silicon-based consolidants/water repellents and on their application [21]. The nanomaterials have been successfully used as antimicrobials for *in situ* experimentation on different stone substrates [22]. Despite the very encouraging results obtained with these nanomaterials, the dark colour of copper may restrain the application possibilities due to possible aesthetic alteration: only low amounts could be used or dark substrates could be treated. The preparation of white-coloured ZnO-NPs and the development of the nanostructured films reported herein represent an interesting improvement for different reasons. First of all these coatings are able to meet the aesthetic requirements for application in the field of cultural heritage. Moreover, the efficacy could be different from metal to metal as a function both of the size and shape of the designed nanomaterial and of the specific target microorganisms resistance to the antimicrobial agent [23]. Despite the well- known efficacy of both copper and zinc nanomaterials in reducing/blocking the growth of a wide range of microorganisms, it has been proved that the antibacterial effect of ZnO–NPs is significantly more pronounced on Gram-positive bacteria than on Gram-negative ones, probably due to their different cell membrane structure [24].

In this study, specific amounts of white ZnO-NPs powder were dispersed in consolidant/water repellent solutions and the resulting dispersions were then spin-coated on glass slides or applied on stone substrates. All the nanocoatings were characterized from the spectroscopic and morphological point of view. Preliminary experiments assessing the ability of the nanomaterials to release zinc were carried out, along with the evaluation of their antimicrobial properties.

Experimental

Nanomaterial preparation

Zinc oxide nanoparticles ~~(ZnO-NPs)~~ were prepared by means of an electrochemical technique. The preparation was carried out in a three-electrode cell configuration with two zinc plates as working and counter electrodes, and Ag/AgCl (KCl sat.) as reference electrode, all immersed in an alkaline solution of $NaHCO_3$ (30 mM) and polystyrene sulphonate (1 g/L) [25, 26]. The electrosynthesis was performed in galvanostatic mode at 10 mA/cm^2 using a PAR 263A potentiostat-galvanostat. After centrifugation the resulting precipitate was dried at 70°C, overnight. The obtained powder was calcined at 600°C in a muffle furnace in air for 1 h. The calcined samples were morphologically characterized by Transmission Electron Microscopy (TEM) with a FEI Tecnai 12 system operating at HV 120 kV.

Estel1000, Estel1100 and Silo111 are ready-to-use silicon-based consolidant/water-repellent materials provided by CTS (Altavilla Vicentina, Italy). According to the technical data sheet Silo111 is a water repellent composed of a mixture of low molecular weight organosiloxane oligomers, Estel1000 is a consolidant composed of tetraethylortosilicate (TEOS), whereas Estel 1100 contains both (TEOS) and siloxane oligomers and is therefore considered to possess both consolidant and water-repellent properties. All materials are dissolved in white spirit D40 (a mixture of hydrocarbons distilled from oil with a boiling point in the range 150–200 °C). The siloxane oligomers are typically composed of dimethyl-siloxanes [27, 28]. TEOS is well known to undergo chemical modifications upon air exposure, leading to loss of ethanol moieties and to various polymerisation phases. In the first step, hydrolysis of ethyl silicate occurs: it reacts with atmospheric/substrate water to produce ethanol and siloxane moieties. The former evaporates while the latter starts to polymerise, leading to silica gel formation which eventually binds to the stone thus consolidating its structure [29]. The ZnO nanocolloids were dispersed in Estel1000, Silo111, and Estel1100 to prepare nanostructured thin films. The procedure consisted in mixing the ZnO-NPs white powder with the consolidant/water-repellent materials at various %w/w concentrations. The resultant dispersions were then spin-coated on glass slides or applied on stone specimens (see below). Nanostructured films loaded with variable amounts of NPs were prepared by simply modifying the mixing ratio of colloidal and polymeric solutions [21, 30, 31].

XPS characterization

Glass slides deposited films of pure Estel1000, pure Silo111, pure Estel1100, Estel1000/ZnO-NPs, Silo111/ZnO-NPs, and

View Article Online
DOI: 10.1039/C5NJ00527B

Estel1100/ZnO-NPs nanocomposites were characterised by means of x-ray photoelectron spectroscopy (XPS), using a Theta Probe VG Scientific spectrometer equipped with a monochromatised AlKα source (spot=300μm). Survey spectra were recorded in constant analyser energy mode (CAE) at a pass energy of 150 eV, while high-resolution regions (C1s, O1s, Si2p, Zn2p) were acquired in CAE mode at a pass energy of 100 eV. Calibration of the Binding Energy (BE) scale was performed by fixing the aliphatic component of the C1s signal at BE values of 284.8±0.1 eV.

Zinc release experiments

Determination of the amount of zinc released from the nanostructured films into nitric acid aqueous contact solution (2% w/w) mimic rainwater was carried out with inductively coupled plasma mass spectrometry (ICP-MS) analyses by means of a Perkin Elmer Elan 9000 spectrometer. 1 mL of solution was deposited onto each modified glass slide; the solution was sampled after a 24 hour contact period and analysed. Zinc was measured on the basis of its isotope 64. Quantification was performed using indium 25 ppb as internal standard.

Biological experiments

The nanocomposites were subject to some bioactive tests using *Aspergillus niger* as target microorganism. This is a very common fungus ubiquitous in soil and commonly reported from indoor and outdoor environments. It was grown on Nutrient Agar (NA) – CM 0003 culture medium incubated at 37°C for 48 hours. Different dilutions (from 10^{-1} to 10^{-9}) were prepared and were then explored in the biological tests in order to choose the best experimental conditions. Nanocomposites modified glass slides were immersed in bottles containing 20 mL of 10^{-5} dilution and incubated at 35 °C for 24 hours. 1 mL of this solution was then plated and after a further period of 24 hours the colonies, if any present, were counted.

Applicative step

Stone samples. Three calcareous buildings stones from Apulia were selected. The first one is Calcare di Altamura (C), a fine-grained biomicrite packstone-wackestone with a rather low porosity, estimated around 3%. The other stones are two varieties of Calcarenite di Gravina: a light yellow, biolitoclastic fine-grained wackestone-packstone from a quarry district in Massafra (M) and a whitish, bioclastic medium-grained packstone from Gravina (G). These materials show a certain similarity in terms of porosity (porosity ranges from ca. 40% (M) to 50% (G)), dry density and uniaxial compressive strenghth, but have different textural features and pore-size distributions. Pore-size diameters of 10-30 μm and 1-10 μm prevail in M, whereas in G pore-size diameters > 30 μm were shown to be the most abundant. Detailed information on the petrophysical and mechanical properties of both calcarenites, including porosity, pore size distribution, density, water absorption, degree of saturation, permeability, thermal properties as well as compressive strength and flexural strength have been reported in literature [32, 33].

Specimens were prepared by cutting square blocks with dimensions of 2.5×2.5×1 cm^3 for the Calcare di Altamura, and quarters of a circle with r = 2.5 cm and thickness of 1 cm for both Calcarenite di Gravina stone types.

The specimens were treated with Estel1000 and Silo111, and with these consolidant/water-repellents loaded with 0.5% w/w of ZnO-NPs. Application of the materials was carried out by brush up to complete imbibition on the specimens, which were then kept at room temperature in order to allow for solvent evaporation and curing of the coating.

Colorimetric measurements. Evaluation of color changes of the treated stone samples was carried out by means of colorimetric measurements using a Konica-Minolta Chroma Metre (CM-2600d). The operating conditions were based on the "Raccomandazioni UNI Normal 43/93" [34]. The results were reported in the CIE-L*a*b* system. For each stone specimen, four (samples C) or three (samples M and G) points of analysis were selected; the instrument was set to automatically give the average value of the colorimetric coordinates (L*, a*, b*) of three measurements for each point. The resultant chromatic change ΔE was determined by means of the following equation: $\Delta E = (\Delta L^2+\Delta a^2+\Delta b^2)^{1/2}$. Then, for each specimen the ΔE values were averaged out to obtain a single value and standard deviation. Measurements were performed on the same points of the specimens by means of a proper mask, before and after the remedy product application.

SEM-EDS analyses. Fragments of all treated and untreated stone specimens were observed with an S360 SEM instrument (Cambridge Instruments) to evaluate the morphological modifications after nanocomposite application. The semi-quantitative elemental composition was obtained using an X-ray energy-dispersive spectrometer (EDS) with an Oxford-Link Ge detector, equipped with a Super Atmosphere Thin Window (ATW) with a thickness of 0.4 mm. An accelerating voltage of 15 keV and a beam current of 500 pA were used. Before SEM–EDS investigations, specimens were coated with a 30 nm conductive graphite film.

Results and discussion

Nanocomposites preparation

ZnO-NPs were prepared according to an electrochemical procedure reported in literature [25] and modified by adding sodium polystyrene sulphonate as stabilizing agent to the electrolytic medium, which resulted in an improved morphology and control of NP growth [26]. A final thermal treatment of the nanocolloid at T = 600°C allowed the complete conversion into nanostructures having a ZnO stoichiometry. A TEM image is reported in Figure 1, where it is possible to observe the presence of nanostructures. The Selected Area Electron Diffraction analysis (data not reported) showed ZnO faceted wurtzite crystallites with an average size of 50 nm.

ARTICLE
View Article Online
DOI: 10.1039/C5NJ00527B
Journal Name

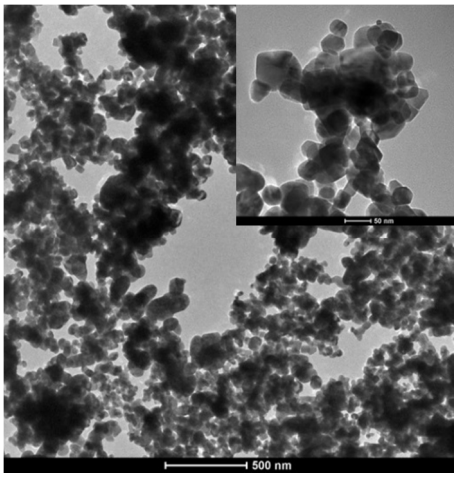

Figure 1. TEM images of electrosynthesized ZnO, after calcination at T=600°C. A magnification is reported in the inset.

Estel1000, Silo111, and Estel1100 were chosen as dispersing media for ZnO-NPs, thanks to their consolidant and water-repellent properties. As already evidenced in the Experimental section, ethylsilicate is well known to undergo chemical modifications upon air exposure, leading to loss of ethanol moieties and to various polymerization phases. This behaviour was taken into consideration by foreseeing a period of at least 40 days of curing time before any characterization and/or use of the nanocomposites [21]. Specific amounts of ZnO-NPs powder were dispersed into the consolidant/water-repellent solution obtaining dispersions with different %w/w of ZnO-NPs.

Nanocomposite surface characterization

Glass slides deposited materials were analysed by means of XPS. Bare Estel1000, Silo111, and Estel1100 along with nanostructured films at different ZnO-NPs bulk concentrations were investigated. The aim was to study the best experimental conditions to yield a viable zinc concentration on the surface of the nanomaterials without affecting the properties of the consolidant/water repellent materials.

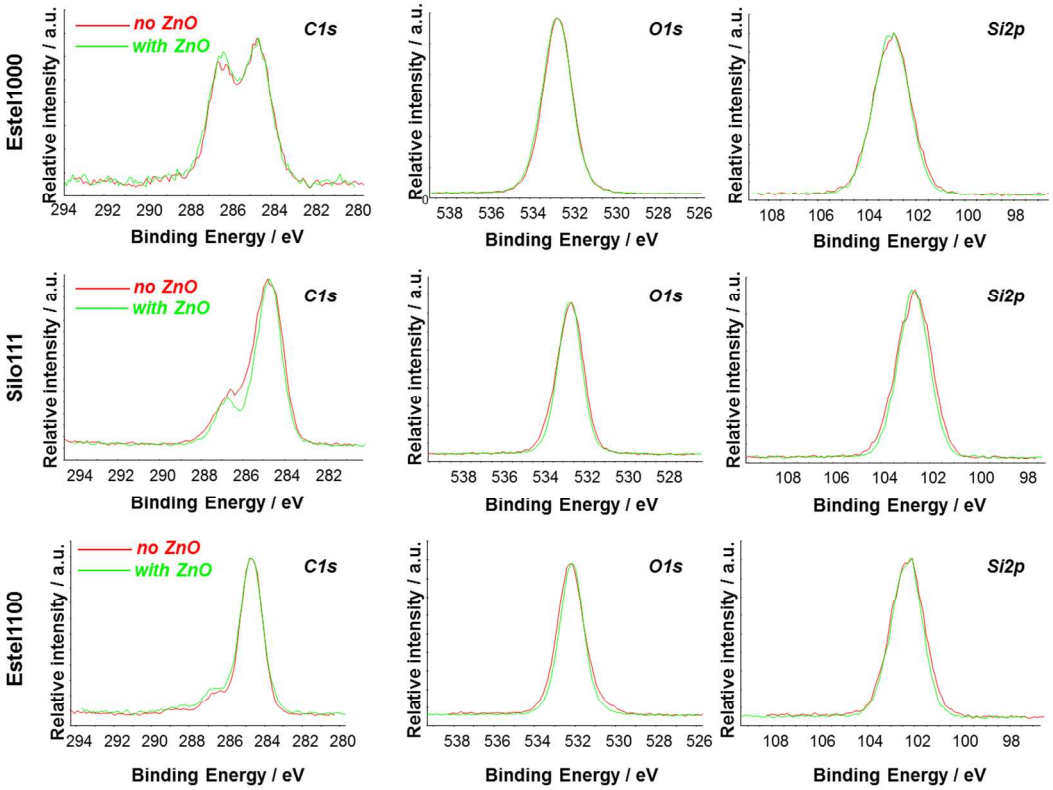

Figure 2. XP spectra of carbon, oxygen, and silicon regions recorded on Estel1000, Silo111, and Estel1100 based coatings; with (green lines) and without (red lines) ZnO-NPs

Journal Name View Article Online DOI: 10.1039/C5NJ00527B ARTICLE

The XPS analyses of the different materials revealed the presence of carbon, oxygen, and silicon, as expected on the basis of the chemical composition. Small amounts of zinc were also detected on the surface of Estel1000 and Estel1100 based nanocomposite materials. In Figure 2 the XP spectra of all spectral regions are reported. The first row of Figure 2 reports the comparison of C1s, O1s, and Si2p spectra for Estel1000 based materials with (green line) and without (red line) ZnO-NPs. The second and third rows report the analogue comparisons for the Silo111-and Estel1100-based nanomaterials. In all cases no differences were found upon ZnO-NPs inclusion and, therefore, it can be stated that embedding of nanoparticles does not significantly change the surface chemistry of the consolidant/water repellents.

As regards the surface availability of ZnO, no zinc could be detected on the top surface of Silo111 nanocomposite films, regardless the curing time and/or the bulk loading of the ZnO-NPs. A possible explanation for this behaviour might be found in the high density of the polysiloxane matrix which, indeed, may not allow the nanoparticles to emerge. On the contrary, XPS analyses performed on Estel1000 and Estel1100 based nanocomposites revealed some zinc on the surface, especially after curing. In Figure 3 the Zn2p XP spectra recorded on the Estel1100/ZnO-NPs composite are reported. This figure clearly shows the zinc surface availability after a 40-day curing period of the film. The spectral region presents the typical doublet peaks: Zn2p3/2 (at lower BE value) and Zn2p1/2 (at higher BE value) components. The zinc is present in a single oxidation state as zinc oxide, so retaining the chemical speciation of the thermally treated ZnO-NPs [26].

A possible dependence of the surface Zn % on the bulk amount was also investigated. The results are reported in Table 1. These data suggest that the bulk concentration does not significantly influence the surface atomic percentage.

Table 1. Surface Zn atomic percentages vs. bulk amount, determined by XPS measurements on composites after 40 days of curing.

% ZnO-NPs w/w	% Zn_{atomic}		
	Estel1000 ZnO-NPs	*Silo111 ZnO-NPs*	*Estel1100 ZnO-NPs*
0.03%	n.d.	n.d.	n.d.
0.15%	n.d.	n.d.	0.3±0.2
0.20%	0.1±0.2	n.d.	0.3±0.2
0.25%	0.4±0.2	n.d.	0.3±0.2

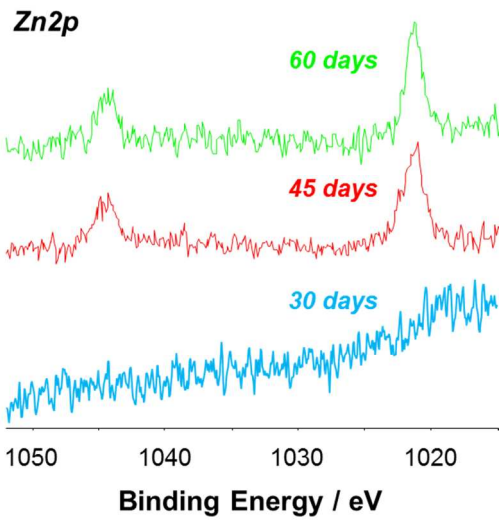

Figure 3. Zn XP spectral region recorded on Estel1100/ZnO-NPs nanocomposite at different curing times

Zinc release experiments

ICP-MS analyses were used to evaluate the zinc release from the prepared nanomaterials into a proper contact solution. An acid aqueous solution was used to mimic the pH condition of rainwater to which stone monuments are usually exposed. Glass slides modified with Estel1000/ZnO-NPs, Silo111/ZnO-NPs, and Estel1100/ZnO-NPs nanocoatings at two different %w/w were covered with the contact solution for 24 hours; after this period the solution was sampled and analysed. The results are reported in Table 2.

Table 2. Zinc amount released by the nanocomposites (curing time 40 days) in nitric acid aqueous solution after a 24 hours contact period.

	Zinc release / ppm	
	ZnO 0.15%w/w	ZnO 0.25%w/w
Estel1000	4.58±0.09	31.6±0.3
Silo111	2.89±0.08	3.60±0.08
Estel1100	0.86±0.06	0.98±0.04

The data suggest that the nanomaterials are able to release zinc amounts in the range of ppm concentration. Moreover, the amount of release seems to be dependent on the bulk

ARTICLE
View Article Online
DOI: 10.1039/C5NJ00527B
Journal Name

concentration for all matrices. Therefore, apparently the metal release process is not strictly influenced by the surface availability but by the bulk concentration; indeed, Silo111 materials show a certain zinc release although no zinc was found on their surfaces by XPS investigation.

Biological experiments

Preliminary biological experiments were performed on Estel1100 nanocomposites in order to study the bioactive properties of ZnO-NPs. *Aspergillus niger* was chosen as target microorganism due to its presence in outdoor environments.
The measurements were performed following the protocol reported in the experimental section. The results are shown in Figure 4.

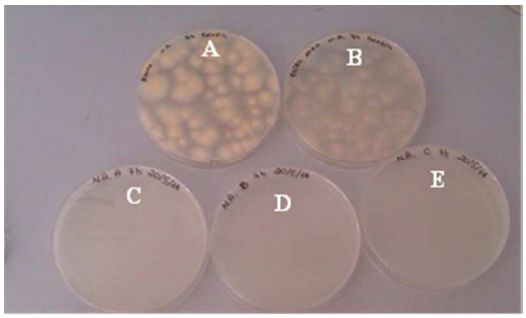

Figure 4. *Aspergillus n*. colonies after 24 hours of contact with nanocomposites covered glass slides. A) control plate; B) Estel1100; C) Estel1100/ZnO-NPs 0.15% w/w; D) Estel1100/ZnO-NPs 0.30% w/w; E) Estel1100/ZnO-NPs 0.60% w/w.

This figure shows the images of the Petri dishes containing the plating of culture broth after 24 hour of contact with the nanocomposites. As can be observed, only the control and bare Estel1100 dishes show the growth of *Aspergillus* colonies, more or less in the same amount. All the other plates are completely disinfected, regardless the ZnO-NPs weight percentage.

Applicative step

After the chemical characterization, release studies, and biological tests, which were performed on the nanocomposites applied on glass slides, an applicative step was undertaken. This step consisted in the study of stone specimens treated with consolidant/water-repellents and relative nanocomposite coatings.
In the field of restoration and conservation of cultural heritage, treatments have to fulfil requirements such as reversibility and compatibility, also from an aesthetic point of view. This means that no significant color change should be observed upon remedy application. In this study whitish zinc oxide nanoparticles were dispersed in colorless consolidant/water-repellents, and thus no significant chromatic changes are to be expected. However, the proper amount of ZnO-NPs able to accomplish its bioactive action without affecting the aesthetics should be assessed. To this purpose colorimetric measurements were performed. Moreover, SEM-EDS analyses were carried out to fully understand the nanocomposite–stone specimen system behavior.
Colorimetric measurements were performed on selected stone samples with different porosity: Calcare di Altamura and two types of Calcarenite di Gravina (from caves in Massafra and Gravina).
Evaluation of chromatic changes of the stone specimens upon application of Estel1000, Silo111, and their relevant nanocomposites containing 0.5% w/w of ZnO-NPs was carried out. The ΔE values obtained immediately after application (at 2 hours) show a consistent decrease after 14 days (data not shown) and diminish substantially after 40 days. This trend was expected since solvent gradually evaporates and the consolidant/water-repellents should have completed curing at that time. The graph in Figure 5 reports the colorimetric data of all treated stone samples at 40 days after application.

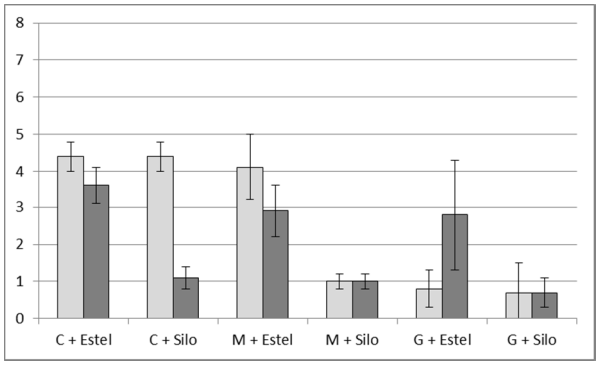

Figure 5. Color changes (ΔE) of Calcare di Altamura (C), Calcarenite di Gravina from Massafra (M), and Calcarenite di Gravina from Gravina (G) specimens treated with Estel1000 and Silo111 (light grey bars) and admixed with ZnO-NPs (0.5% w/w) (dark grey bars) measured at 40 days after application.

Examination of these data leads to the following conclusions. Significant differences can be observed between the three types of stone substrates. In particular, all samples composed of Calcare di Altamura (C) show the highest ΔE values, although all below 4.5. The more porous Calcarenite di Gravina samples (M and G) exhibit minor chromatic changes, which is probably due to a better absorption/penetration of the applied materials. Comparison between the behaviour of pure Estel1000 and Silo111 reveals that the former generates more significant color changes than the latter. It should be evidenced, however, that the addition of ZnO-NPs seems to attenuate the chromatic variations induced by application of Estel1000 and Silo111, at least on the C substrate. In the other case the admixing of ZnO-NPs does not substantially change the coatings colour. An exception is the G stone specimens treated with Estel1000 and

View Article Online
DOI: 10.1039/C5NJ00527B

Estel1000/ZnO-NPs, which is probably due to the non-homogeneous composite distribution on the specimen, caused by the high surface roughness of this stone substrate.

These results represent a very interesting improvement with respect to the use of copper-based coatings, since the highest ΔE values in this study are all lower than 5, despite the amount of embedded ZnO–NPs is much higher. Indeed, a fourfold reduction of the ΔE values is observed for all the stone substrates even if using a tenfold ZnO–NPs %w/w with respect to CuNPs [21].

SEM-EDS analyses were performed on fragments which were detached from the surface of the stone specimens treated with Estel1000, Silo111, Estel1000/ZnO-NPs (0.5% w/w), and Silo111/ZnO-NPs (0.5% w/w). For each sample, three backscattered electron (BSE) images at different magnifications - 150 x, 750 x, and 2000 x - were acquired, as well as an ED raster spectrum for elemental analysis. The fragments composed of Calcare di Altamura (C) show a homogeneous and compact surface with low porosity. EDS data indicate a prevalence of calcium carbonate with low contents of silicon and magnesium. Treatment with Silo111 and Estel1000 seems to provide a more homogeneous surface as compared with the untreated samples. Microchemical analyses revealed a higher relative amount of silicon for Estel1000 as compared with Silo111, pointing to a better absorption of the latter product. When admixed with ZnO-NPs, Estel1000 shows some cracking, which is clearly visible in the BSE image and which is more pronounced in correspondence to large grains. Similarly, the compact C stone specimen treated with Silo111/ZnO-NPs is characterized by homogeneously diffused whitish areas with a very high concentration of 5 µm clusters rich in zinc and silicon (Figure 6A). In some interstices Silo111 has formed amorphous characteristic structures. The relative amount of zinc with respect to calcium and silicon is lower in the Silo111 sample as compared to the Estel1000 sample.

Regarding the stone specimens of Calcarenite di Gravina from Massafra (M), the acquired BSE images allow to confirm the observations made with optical microscopy. This stone is less compact than the previous limestone and is mainly composed of calcium carbonate with significant amounts of magnesium, aluminium and silicon. While the latter two elements can be probably ascribed to the presence of clay minerals, the occurrence of magnesium is most likely to be attributed to dolomite. The BSE images of the treated specimens evidenced a homogeneous distribution of Silo111 and Estel1000. As for the Calcare samples, the ED raster spectra show a higher concentration of silicon on the surface of the Estel1000 samples with respect to those treated with Silo111. In the SEM-BSE image of the Estel1000/ZnO-NPs treated M sample, the luminous zinc particles can be clearly observed. As previously remarked for the C specimen, the consolidant tends to concentrate in specific areas containing zinc oxide aggregates (2-20 µm) and showing cracking (Figure 6B). In Figure 6C the ED raster spectrum is reported. Application of Silo111/ZnO-NPs produces a fairly good distribution of the water-repellent as well as of the zinc oxide, which is present as single crystals and agglomerates. Again, the relative content of zinc with respect to the other main elements was found to be lower in the Silo111 sample with respect to the Estel1000 sample.

SEM analyses confirm the high porosity of the Calcarenite di Gravina from the Gravina cave (G), achieving 45%. This should be taken into account when evaluating the penetration capacity of the applied materials like the consolidant/water-repellents used in this study.

Microanalyses indicate the presence of calcium carbonate as well as of clay minerals. Again, SEM investigation evidenced a higher amount of silicon on the surface for the Estel1000 samples with respect to the Silo111 ones.

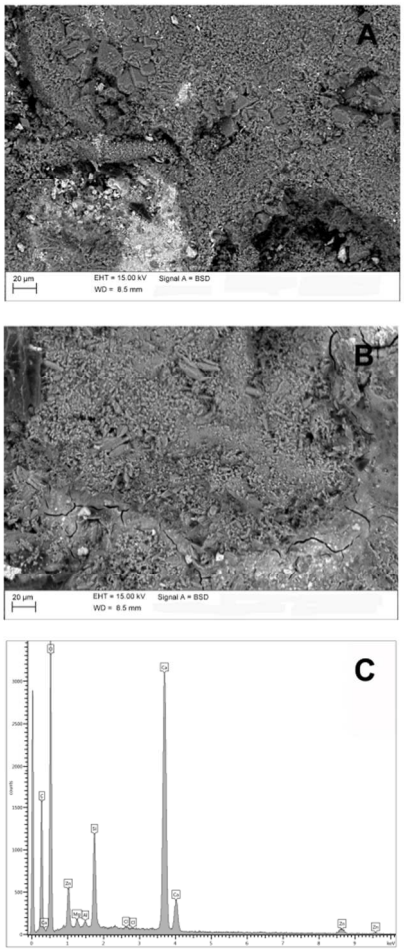

Figure 6. SEM-EDS analyses of stone specimens. A) BSE image of Calcare di Altamura treated with Silo111/ZnO-NPs; B) BSE image of Calcarenite di Gravina from Massafra treated with Estel1000/ZnO-NPs and C) its relative raster ED spectrum.

The BSE image of the sample treated with Estel1000 shows that the consolidant is present in the cavities as amorphous pseudocrystalline material. The ED raster spectrum acquired on the Estel1000/ZnO-NPs treated specimen shows a rather high amount of silicon and few zinc, which is however well distributed in small aggregates with dimensions ranging from 1 to 20 µm. Concerning the application of Silo111/ZnO-NPs,

ARTICLE
View Article Online
DOI: 10.1039/C5NJ00527B
Journal Name

SEM-BSE images show an even distribution of 1-10 µm zinc grains on the surface of the calcarenite. In this case, the zinc peak of the ED spectrum is higher than that for silicon, contrary on what was previously observed for the C and M samples.

Conclusions

In this study, the ability of zinc oxide nanoparticles to exert biocide activity when embedded in commonly used consolidant/water repellent materials has been demonstrated. X-ray photoelectron spectroscopy showed that the presence of the nanoparticles did not affect the surface chemistry of the matrices. The surface or sub-surface availability of zinc was also assessed. For the Estel1000 and Estel1100-based materials the amount of Zn was shown to increase in the surface region with curing, whereas zinc remains confined within the sub-surface region in Silo111-based composites. Preliminary release data suggested, however, that zinc was released in acid contact solutions independently from its top surface availability. Diffusion of nanoparticles from the bulk to the contact solution is a plausible mechanism. Biological tests with *Aspergillus niger* evidenced remarkable biostatic activity of the tested nanocomposites, even at rather low ZnO loadings. Therefore, we can state that the prepared nanomaterials are able to embed zinc oxide nanoparticles and to release zinc in order to exert interesting bioactive properties. Application of the ZnO nanocomposites on calcareous stone specimens was shown to generate acceptable chromatic variations. The scanning electron microscopy with X-ray microanalysis measurements, performed on the single consolidant and water repellent, seem to confirm the surface spectroscopy data in that the relative amount of zinc is lower on the surface of the samples treated with Silo111 as compared to the Estel1000 ones. The mixed matrix, Estel1100, is expected to show a mixed behaviour. All the nanocomposites proved to be stable, since morphological and surface chemical analyses performed after more than one year show results similar to those obtained soon after the application. Moreover, no detachment of the coatings has been observed after such a period. In perspective, kinetic measurements will be set and performed to evaluate long-lasting zinc release capability of the nanocoatings. ~~and~~ *In situ* experiments have been started with the application of Estel1100/ZnO-NPs and Silo111/ZnO-NPs: after six months no colonization could be observed neither on the treated nor on the control areas. This was expected since biological colonization may take a very long time. Moreover, the biocide activity tests will be extended to different microorganisms usually present in the biological community colonizing stone substrates.

Acknowledgements

The authors would like to thank Prof. Pasquale Acquafredda (Dipartimento di Scienze della Terra e Geoambientali, Università degli Studi di Bari "Aldo Moro", Italy) for petrographic characterization and for his precious assistance in the SEM-EDS analyses, and Mr. Simoncarlo Giacummo for his valuable support in the XPS analyses. This work was performed in the framework of the PRIN 2010-11 "Sustainability in cultural heritage: from diagnosis to the development of innovative systems for consolidation, cleaning and protection" code 2010329WPF, funded by MIUR. The authors are grateful to the projects PO Puglia FESR 2007-13 “RESTAUREO” (3Z3VZ46) and PON03 “MAIND” (PE0004) for partial financial support.

Notes and references

[a] Dipartimento di Chimica, Università degli Studi di Bari "Aldo Moro", via Orabona 4, 70125 Bari–Italy.
[b] Centro Interdipartimentale "Laboratorio di ricerca per la diagnostica dei Beni Culturali", Università degli Studi di Bari "Aldo Moro", via Orabona 4, 70125 Bari–Italy.
[c] Dipartimento di Medicina Veterinaria, Università degli Studi di Bari "Aldo Moro", Strada prov.le per Casamassima km. 3, Valenzano (BA)–Italy
*corresponding authors

1 N.C.T. Martins, C.S.R. Freire, C.P. Neto, A.J.D. Silvestre, J. Causio, G. Baldi, P. Sadocco and T. Trindade, *Colloid Surface A*, 2013, **417**, 111.
2 T. Gordon, B. Perlstein, O. Houbara, I. Felner, E. Banin and S. Margel, *Colloid Surface A*, 2011, **374**, 1.
3 N. Jones, B. Ray, K.T. Ranjit and A.C. Manna *Fems Microbiol. Lett.*, 2008, **279**, 71.
4 L. Huang, D.Q. Li, Y.J. Lin, M. Wei, D.G. Evans and X. Duan, *J. Inorg. Biochem.*, 2005, **99**, 986.
5 F.R. Marciano, D.A. Lima-Oliveira, N.S. Da-Silva, A.V. Diniz, E.J. Corat and V.J. Trava Airoldi, *J. Colloid Interf. Sci.*, 2009, **340**, 87.
6 L.L. Zhang, Y.H. Jiang, Y.L. Ding, N. Daskalakis, L. Jeuken, M. Povey, A.J. O’Neill and D.W. York, *J. Nanopart. Res.*, 2010, **12**, 1625.
7 R. Wahab, A. Mishra, S.I. Yun, Y.S. Kim and H.S. Shin, *Appl. Microbiol. Biot.*, 2010, **87**, 1917.
8 A. Lipovsky, Y. Nitzan, A. Gedanken, R. Lubart, *Nanotechnology*, 2011, **22**, 105101.
9 S. Selvam and M. Sundrarajan, *Carbohyd. Polym.*, 2012, **87**, 1419.
10 C. Karunakaran, V. Rajeswari and P. Gomathisankar, *J. Alloy Compd*., 2010, **508**, 587.
11 N. Padmavathy and R. Vijayaraghavan, *Sci. Technol. Adv. Mat.*, 2008, **9**, 035004.
12 T.J. Mccarthy, J.J. Zeelie and D.J. Krause, *J. Clin. Pharm.Ther.*, 1992, **17**, 51.
13 J.J. Zeelie and T.J. McCarthy, *Analyst*, 1998, **123**, 503.
14 H. Zhou, X. Wang, Y. Zhou, H. Yao and F. Ahmad, *Anal. Bioanal. Chem.*, 2014, **406**, 3689.
15 O.M. El-Feky, E.A. Hassan, S.M. Fadel and M.L. Hassan, *J. Cult. Herit.*, 2013, **15**, 165.
16 L. Lazzarini, M. Laurenzi Tabasso, *Il restauro della pietra*. Padova: CEDAM; 1994
17 J. Delgado-Rodrigues, Consolidation of decayed stones: a delicated problem with few practical solutions, in: P.B. Lourenço, P. Roca (Eds.), Proceedings of 3rd International Seminar on Historical Constructions, Universidade do Minho, Guimarães, 2001, pp. 3–14.

View Article Online
DOI: 10.1039/C5NJ00527B

18 R. Zárraga, J. Cervantes, C. Salazar-Hernandez, G. Wheeler, *J. Cult. Herit.*, 2010, **11**, 138.
19 G. Wheeler, Alkoxysilanes and the consolidation of stone, The Getty Conservation Institute, Research in Conservation, Los Angeles, 2005.
20 C. Rodriguez-Navarro, E. Doehne, *Earth Surface Processes and Landforms*, 1999, **24**, 191.
21 N. Ditaranto, S. Loperfido, I. D. van der Werf, A. Mangone, N. Cioffi and L. Sabbatini, *Anal. Bioanal. Chem.*, 2011, **399**, 473.
22 D. Pinna, B. Salvadori and M. Galeotti, *Sci. Total Environ.*, 2012, **423**, 132.
23. D. Longano, N. Ditaranto, L. Sabbatini, L. Torsi and N. Cioffi in Nano-Antimicrobials. Progress and Prospects. N. Cioffi and M. Rai Eds. Springer 2012.
24. A. C. Manna in Nano-Antimicrobials. Progress and Prospects. N. Cioffi and M. Rai Eds. Springer 2012.
25 K.G. Chandrappa, T.V. Venkatesha, K. Vathsala and C. Shivakumara, *J. Nanopart. Res.*, 2010, **12**, 2667.
26 M.C. Sportelli, D. Hötger, R.A. Picca, K. Manoli, C. Kranz, B. Mizaikoff, L. Torsi and N. Cioffi, *MRS Online Proceedings Library*, 2014, **1675**, mrss14-1675-k05-04, doi: 10.1557/opl.2014.847.
27. E. Tesser, F. Antonelli, L. Sperni, R. Ganzerla and N.P. Maravelaki, *Polym. Degrad. Stabil,* 2014, **110**, 232.
28. L. Téllez, J. Rubio, F. Rubio, E. Morales and J.L. Oteo, *Spectrosc. Lett.*, 2004, **37**, 11.
29. F. Rubio, J. Rubio and J.L. Oteo, *Spectrosc. Lett.*, 1998, **31**, 199.
30 N. Cioffi, L. Torsi, N. Ditaranto, L. Sabbatini, P.G. Zambonin, G. Tantillo, L. Ghibelli, M. D'Alessio, T. Bleve-Zacheo and E. Traversa, *Appl. Phys. Lett.*, 2004, **85**, 2417.
31 N. Cioffi, L. Torsi, N. Ditaranto, G. Tantillo, L. Ghibelli, L. Sabbatini, T. Bleve-Zacheo, M. D'Alessio, P.G. Zambonin and E. Traversa, *Chem. Mater.*, 2005, **17**, 5255.
32 G.F. Andriani, N. Walsh, Geological Society, London, Special Publications, 2007, **271**, 179.
33 G.F. Andriani, N. Walsh, Geological Society, London, Special Publications 2010, **333**, 129.
34 Raccomandazioni NorMal 43/93, 1993, Rome. CNR-ICR.